Biomarkers, 2012; 17(3): 223–230
© 2012 Informa UK, Ltd.
ISSN 1354-750X print/ISSN 1366-5804 online
DOI: 10.3109/1354750X.2012.657245

informa
healthcare

RESEARCH ARTICLE

Comparison of plasma from healthy nonsmokers, smokers, and lung cancer patients: pattern-based differentiation profiling of low molecular weight proteins and peptides by magnetic bead technology with MALDI-TOF MS

Syed G. Musharraf[1,2], Naghma Hashmi[2], M. Iqbal Choudhary[1,2], Nadeem Rizvi[3], Ahmed Usman[3], and Atta-ur-Rahman[1,2]

[1]*Dr. Panjwani Center for Molecular Medicine and Drug Research,* [2]*H.E.J. Research Institute of Chemistry, International Center for Chemical and Biological Sciences, University of Karachi, and* [3]*Jinnah Postgraduate Medical Center, Karachi, Pakistan*

Abstract

Context: Smoking is the major contributor of lung cancer (LC), which accounts for millions of death.

Objective: This study focused on the correlation between the proteomic profiling of LC patients, and healthy nonsmokers and smokers.

Method: Pattern-based peptide profiling of 186 plasma samples was performed through reversed-phase chromatography-18 magnetic bead fractionation coupled with matrix-assisted laser desorption/ionization time-of-flight mass spectrometry analysis and resulted data were evaluated statistically by ClinProTool.

Results: Marker peaks at m/z 1760, 5773, 5851, 2940, and 7172 were found with an excellent statistical figure.

Conclusion: Selected marker peaks can be served as a differentiated tool of LC patients with high sensitivity and specificity.

Keywords: C-18 magnetic bead, ClinProTools software, MALDI-TOF-MS, smokers, lung cancer, plasma peptide, pattern-based profiling

Introduction

Lung cancer (LC) is a lethal disease worldwide (Jemal et al. 2010), responsible for 28% of all cancer deaths and approximately 1.3 million deaths worldwide every year (Mascaux et al. 2010). In Asian countries, particularly in Pakistan, LC is the major killer in men, and the death rate has increased in the last few years, with the increasing number of smokers (S) (GLOBOCAN, 2008, Jacobs et al., 1999). Compared with nonsmokers (NS), S show a 30-fold increased risk of developing cancer (Sasco et al. 2004, Proctor, 2001, Walser et al. 2008), and hence, the majority of the new LC diagnosis occurs in former S.

Recent developments in the fields of mass spectrometry and bioinformatics have started a new era for biomarker discovery that can consistently and precisely predict outcomes during cancer management and treatment. Two approaches, namely biomarker discovery and pattern-based diagnostic development, have been utilized in the proteomic analysis. In the biomarker discovery approach, multidimensional fractionation techniques, coupled with MS/MS are used to identify differential proteins/peptides between diseased subjects and matched healthy controls. However, this approach is time-consuming and lacks sensitivity and specificity when applied to large heterogeneous

Dedicated to the memories of my beloved sister, Mrs. Nighat Shahwar died in 2006 due to cancer.

Address for Correspondence: Syed G. Musharraf, H.E.J. Research Institute of Chemistry, International Center for Chemical and Biological Sciences, University of Karachi, Karachi 75270, Pakistan. Tel: +92 213 4824924-5, 4819010; Fax: + 92 213 4819018-9. E-mail: musharraf1977@yahoo.com

(Received 06 November 2011; revised 07 January 2012; accepted 10 January 2012)

population. Biomarker pattern-based diagnosis, due to its high throughput nature, is an emerging technology aimed at overcoming these limitations. Moreover, different fractionation techniques in proteomics profiling greatly improve the biomarker pattern identification. A magnetic bead-based proteomic fingerprinting is the most recent high throughput approach as its functionalized or activated surfaces (much larger than traditional solid protein chips) allow offline fractionation/enrichment of the proteins/peptides present in the biological fluid with high efficiency before MS analysis (Flanagan, 2007). The combination of magnetic bead purification and matrix-assisted laser desorption/ionization time-of-flight mass spectrometry (MALDI-TOF-MS) is a convenient, fast, efficient, and reproducible method for proteomic profiling of serum samples in the mass range of *m/z* 1000–10,000 Da (Sven et al. 2005) and has already been applied to the investigation of biomarkers in various diseases (Wong et al. 2010. Chang et al. 2006, Cheng et al. 2005, Freed et al. 2008, Villanueva et al. 2004. Villanueva et al. 2006a, Villanueva et al. 2006b, Goldman et al. 2007), as a powerful alternative to the surface-enhanced laser desorption ionization approach (Orvisky et al. 2006).

This study is focused on a correlation between the proteomic profiling of LC patients, and healthy NS and S using high-throughput magnetic bead-based approach coupled with MALDI-TOF-MS. Similar studies have been recently published (Shevchenko et al. 2010. Lin et al. 2010) by utilizing weak cation exchange (WCX) magnetic beads. Utilization of C-18 chemistry of magnetic beads for LC comparison with two controls (healthy NS and S) showed interesting results, which are reported here for the first time.

Experimental

Chemicals and reagents

Chemicals and solvents used were of high-performance liquid chromatography (HPLC) grade. Deionized water (Milli-Q) was used throughout the study (Millipore, Billerica, MA, USA). Alpha-cyano-4-hydroxycinnamic acid (HCCA) and trifluoroacetic acid (TFA) were purchased from Aldrich-Sigma (St. Louis, MO, USA). Diammonium citrate, n-octylglucoside, sodium chloride (NaCl), and acetonitrile were purchased from Merck Chemicals (Darmstadt, FR Germany). Protein ladder, reversed-phase chromatography-18 (RPC-18) dynabeads, and dynabead magnetic particle concentrator (Dynal MPC) were from Invitrogen (Dynal AS, Oslo, Norway). NuPAGE 12% precast gel and 2-(*N*-morpholino)-ethanesulfonic acid (MES) running buffer were purchased from Invitrogen (Carlsbad, CA USA).

Patients and control

This study was approved by the ethical committee of Jinnah Postgraduate Medical Center (JPMC), and written informed consent was obtained from all the participants. A total of 186 plasma samples of males were included in this study, among them 120 in the training set (40 from each group in the age range of 30–65 years among S and NS, while 35–70 years in the case of cancer patients) and 66 in the test set (36 NS, 15 S, and 15 LC patients). Cancer subjects included in this study were of pathologically proven LC of common subtypes, particularly nonsmall cell lung cancer mainly at stage III ($n = 12$) and IV ($n = 38$) and were untreated. And, the S included in this study have been smoking for at least 10 years or more.

Biological samples

Blood samples were collected, processed, and stored according to the human proteome organization standard protocol (Rai et al. 2005). About 4 mL of the blood was drawn from the fasting patient in BD vacutainer tubes containing K_2-ethylenediaminetetraacetic acid as an anticoagulant. Plasma was separated by centrifugation at $2200 \times g$ for 10 min at 4°C. Finally, the plasma was aliquoted and frozen at –80°C. The plasma concentration was determined using bicinchoninic acid protein assay kit (Pierce Chemical, Rockford, IL, USA).

Sample fractionation using dynal–C18 magnetic beads

Dynal magnetic bead-based processing was carried on the basis of previously optimized procedure (Jimenez et al. 2007). According to the protocol, 20 μL of the plasma were premixed with 40 μL of the binding buffer (0.15% n-octylglucoside/0.5% TFA) in Eppendorf tubes. For equilibration of the bead slurry, 20 μL of the homogenous magnetic particle solution and 180 μL of 200 mM NaCl/0.1% TFA were transferred to each well of a 96-well microplate. The plate was then placed on Dynabead magnetic particle concentrator (Dynal MPC; Invitrogen) for 20 sec and the supernatant was aspirated. The procedure was repeated twice. The microplate was removed from the MPC device, and 60 μL of the premixed plasma containing binding solution was added and gently mixed with the magnetic beads. After 2 min, the supernatant was collected in a clean Eppendorf tube for sodium dodecyl sulfate-polyacrylamide gel electrophoresis (SDS-PAGE) analysis. Washing was done by carefully mixing 200 μL of 0.1% TFA with the beads and moving the plate back and forth on the MPC device to ensure complete washing. After 30 sec, the supernatant was discarded, and the entire washing procedure was repeated three times. After the final washing step, the bound peptides and proteins were eluted by incubation with 20 μL of 50% acetonitrile (ACN) for 2 min using a magnetic separator. All samples were processed and analyzed on the same day.

One-dimensional SDS-PAGE analysis

SDS-PAGE analysis was performed on X Cell Sure Lock™ Novex mini-cell (Invitrogen), and the analysis was carried out for a single sample from each of the three study group. For this, the eluted protein sample from the five consecutive cycle of Dynabead procedure of the same sample were pooled (20 μL from each cycle and a total of 100 μL obtained from five such cycles), dried by speed-vac (Eppendorf, Hamburg, Germany), and reconstituted

with 12 µL of the reducing sample running buffer. The flow through (unbound) fractions of each of the five cycles of Dynabead was also pooled (approximate volume of about 300 µL) and concentrated on speed-vac till 50 µL, 0.4 µL of this concentrated fraction was mixed with 11.6 µL of the sample reducing buffer. Bound and unbound fractions were separated with the NuPAGE 12% precast gel (Invitrogen) at a constant volt of 200 V. MES was used as a running buffer, and the protein bands were stained by Coomassie Brilliant Blue Staining Kit (Invitrogen, USA).

MALDI-TOF-MS analysis

MALDI analysis was performed on MALDI-TOF-TOF MS (Ultraflex III; Bruker Daltonik GmbH, Breman, Germany) instrument. Samples were spotted on the ground steel target, an aliquot of 0.5 µL of the eluted sample was mixed with 0.5 µL of the matrix (saturated solution of HCCA, in ACN/10 mM diammonium citrate 8:2), allowed to dry and co-crystallized. Plasma mass spectrometric profile was obtained by Flex Control Software (version 3.0). The mass spectrometer was externally calibrated in the reflector positive mode between *m/z* 750–5000 using peptide calibration standard I (Bruker Daltonics). A 337-nm nitrogen laser and a 2-GHz digitizer were used. Spectra were acquired in linear positive mode with 25 KV of ion acceleration, 6 KV of lens potential, and high gating strength to deflect ions with a mass below 800 *m/z*. Delayed extraction was applied at 100 ns, the detector gain was set to 7.5, and the sample rate to 0.5 GS/s. Spectra were acquired in the mass to charge (*m/z*) range of 800–10,000. Each spectrum was the sum of 2000 laser shots randomized over different positions within the same spot (200 shots/position) at a laser frequency of 100 Hz and a laser intensity of 60%–70%. Method repeatability and reproducibility was performed by the analysis of selected samples from the each class on the same day (intra-day) and on different day (inter-day), respectively.

Bioinformatics analysis

MALDI-TOF-MS spectra were analyzed by using flex analysis and ClinProTool (CPT) software (version 2.3) both from Bruker Daltonics for proteomic pattern recognition. The whole data pretreatment including recalibration, normalization, and baseline subtraction were completed using default settings and was performed automatically by the software. This pretreated data were then used for visualization and statistical analysis. The optimal setting for CPT was found to be a signal-to-noise threshold of 5, a Top Hat baseline subtraction with 10% as minimal baseline width and a resolution of 800. Intensities were used for peak calculation and *p* value *T*-test/analysis of variance (ANOVA) for peak selection. Cross validation was performed in random mode with 20% to leave out and 10 number of iterations. For genetic algorithm, number of neighbors was three with automatic detection having a 0.20 mutation rate and a cross over rate of 0.50, and support vector machine (SVM) algorithm calculated with automatic detection of peak having three number of neighbors. For supervised neural network (SNN) model, upper limit of cycles was selected at 30 with an automatic detection of prototype number, while quick classifier was calculated on the basis of *p* value *T*-test/ANOVA as the sort/weight mode.

Results and discussion

This study investigated the diagnostic pattern identification of 186 male plasma samples divided into training set and a test set ($n=66$ comprising of 36 NS, 15 S, and 15 LC), fractionated by magnetic bead RPC-18. However, sequential elution with different concentrations of acetonitrile has been tried and found to be best at 50% of acetonitrile. The resulted eluate was then subjected to mass spectral analysis followed by statistical evaluation. Training set data were subjected to the diagnostic model development, and the selected models were applied for the external and internal validation. MALDI mass spectra of each class were very consistent as shown by stack view (See Supplementary Data Figure 1). However, the reproducibility and repeatability of MALDI spectra as a diagnostic tool has already been investigated in detail by Yildiz et al. (2007). Moreover, coefficient of variance within each group was found to be 0.056, 0.108, 0.067, and 0.050 for groups I, II, III, and IV, respectively. Overall, all three classes can be visualized in gel view (Figure 1).

Differential and statistical analysis of all the data from spectra were analyzed extensively by CPT software. Sample statistics were performed in groups. Group I consisted of NS versus LC, group II of S versus LC, group III of NS versus S, and group IV included the comparison of NS versus S versus LC. CPT provides a list of peaks in the training set selected according to the statistical significance to differentiate between the groups. A total of 141 peaks in group I, 130 in group II, 148 in group III, and 150 peaks in

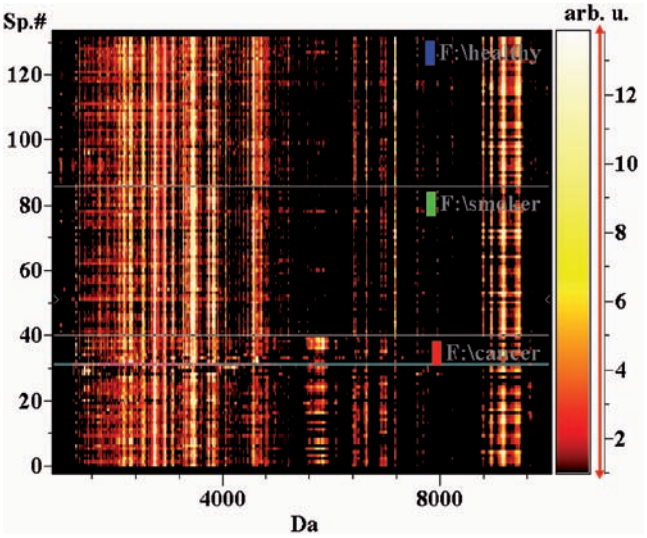

Figure 1. Comparative gel view of the three classes comprises of 120 mass spectra of 40 of each class of nonsmokers, smokers, and lung cancer patients.

group IV between the mass range of *m/z* 900–10,000 were identified (See Supplementary Data Figure 2).

Construction and validation of the diagnostic model

A protein/peptide was considered to be differentially expressed in a group if, when compared with the normal group, statistically significant differences in its intensity were observed ($p < 0.001$). Using a highly sophisticated mathematical algorithm, the CPT software generated models containing several peaks that allow discrimination between spectra sets. Results obtained from each model and a comparison of the different mathematical algorithm for the four study groups are summarized in Table 1. Groups I and II showed the highest value of cross validation >93%, while recognition capability was >96% for all the four algorithms because these were the most discriminative groups. For groups III and IV, the values of cross validation were in the range of 64%–87%, while recognition capability was between 74%–98% because NS and S groups were not so discriminative. On the basis of this internal validation, the SVM has been selected as the best predictive model showing the highest level of cross validation for groups I, II, and III corresponding to 96.7%, 94.3%, and 85.6%, respectively, while the SNN model showed 87.8% for group IV. The recognition capability for group I and II were of 100%, and 96.7% and 94.9% for group III and IV, respectively.

External validation, similar to the cross validation, measures the predictive capability (sensitivity and specificity) of a calculated model. The proposed peak pattern in a model was used to externally validate an independent or blind-test set of 66 plasma samples (36 healthy, 15 S, and 15 LC patients). In group I, the SVM classifier correctly predicted the presence of LC in 15 out of 15 spectra, and 25 healthy out of 36 resulting with 100% sensitivity 71% specificity. In group II, 15 of 15 cancerous and 15 of 15 S have been correctly predicted giving a 100% sensitivity and 100% specificity. Similarly, for group III, 100% sensitivity and 77.1% specificity were achieved by identifying 15 of 15 S and 27 of 36 nonsmoker spectra (See Supplementary Data Table 1). A receiver operating characteristic curve for selected diagnostic peaks with their area under the curve (AUC) values for group I could be seen in Figure 2.

Identification of biomarker pattern

This study generated a differential pattern depending on the specific peaks in various groups. Qualitative analysis of the SVM model for group I showed seven characteristic peaks, picked by the model, possessed authentically to a significant level of *p* value ($p < 0.001$) with an AUC range of 0.857–0.990. Similarly, the qualitative composition of SVM model for group II comprises 17 peaks with *p* values ($p < 0.001$) and AUC range of 0.5097–0.9923 except one peak. Twenty five peaks have been demonstrated in the SVM model for group III among which four peaks have the $p > 0.001$, while the rest of the 21 peaks have $p < 0.001$, AUC in this group ranging from 0.565–0.845 in which three peaks have AUC < 0.6. SNN-based model for group IV identified 23 peaks with only two peaks with higher *p* values and the rest of the peaks have $p > 0.001$ (See Supplementary Data Table 2–5).

A summary of the peaks generated by the SVM model and their overlapping among the three study groups have been shown in Venn diagram (Figure 3). The generated SVM model peaks were overlapped among the three groups, group I showed 85.7% and 57.1% overlapping with group II and III, respectively. Group II showed 35.29% and 17.64% overlapping with groups I and III, respectively, while 16% and 12% overlapping of group III with I and II, respectively, were observed. Among the seven and the seventeen peaks generated by the model for groups I and II, respectively, six peaks at *m/z* 1760, 2117, 2940, 2962, 4571, and 7172 Da were common between groups I and II, while 25 peaks selected by the model for group III showed four common peaks at *m/z* 2117, 2538, 2940, and 2962 Da between groups I and III, and three peaks at *m/z* 2117, 2940, and 2962 Da for groups II and III. The number of peaks that were similar among the three study groups was at *m/z* 2117, 2940, and 2962 Da. Among these three peaks, the peak at *m/z* 2962 Da showed the AUC value below the significant

Table 1. Statistically generated models for the four groups.

Group 1: Nonsmokers vs. Lung cancer						Group II: Smokers vs. Lung cancer					
		Validation						Validation			
Name	Algo	XVal	X1	X2	Rec. Cap.	Name	Algo	XVal	X1	X2	Rec. Cap
GA	GA	96.40%	95.80%	97.00%	97.80%	GA	GA	97.40%	95.80%	99.00%	100%
SVM	SVM	96.70%	94.40%	99.00%	100%	SVM	SVM	94.30%	91.50%	97.00%	100%
SNN	SNN	96.70%	98.60%	94.80%	100%	SNN	SNN	93.00%	89.00%	96.90%	100%
QC	QC	93.80%	87.60%	87.60%	96.70%	QC	QC	94.20%	98.60%	89.70%	98.80%
Group III: Nonsmokers vs. Smokers						Group IV: Nonsmokers vs. Smokesr vs. Lung cancer					
		Validation						Validation			
Name	Algo	XVal	X1	X2	Rec. Cap.	Name	XVal	X1	X2	X3	Rec. Cap.
GA	GA	74.60%	70.40%	78.80%	92.20%	GA	64.80%	72.70%	55.30%	66.30%	81.40%
SVM	SVM	85.60%	91.40%	79.80%	96.70%	SVM	72.80%	84.40%	71.80%	62.20%	92.40%
SNN	SNN	81.50%	72.30%	90.70%	97.80%	SNN	87.80%	93.60%	89.30%	80.60%	94.90%
QC	QC	78.30%	78.30%	78.40%	83.70%	QC	68.00%	97.40%	46.40%	60.20%	74.60%

GA, genetic algorithm; SVM, support vector machine; SNN, supervised neural network; QC, quick classifier.

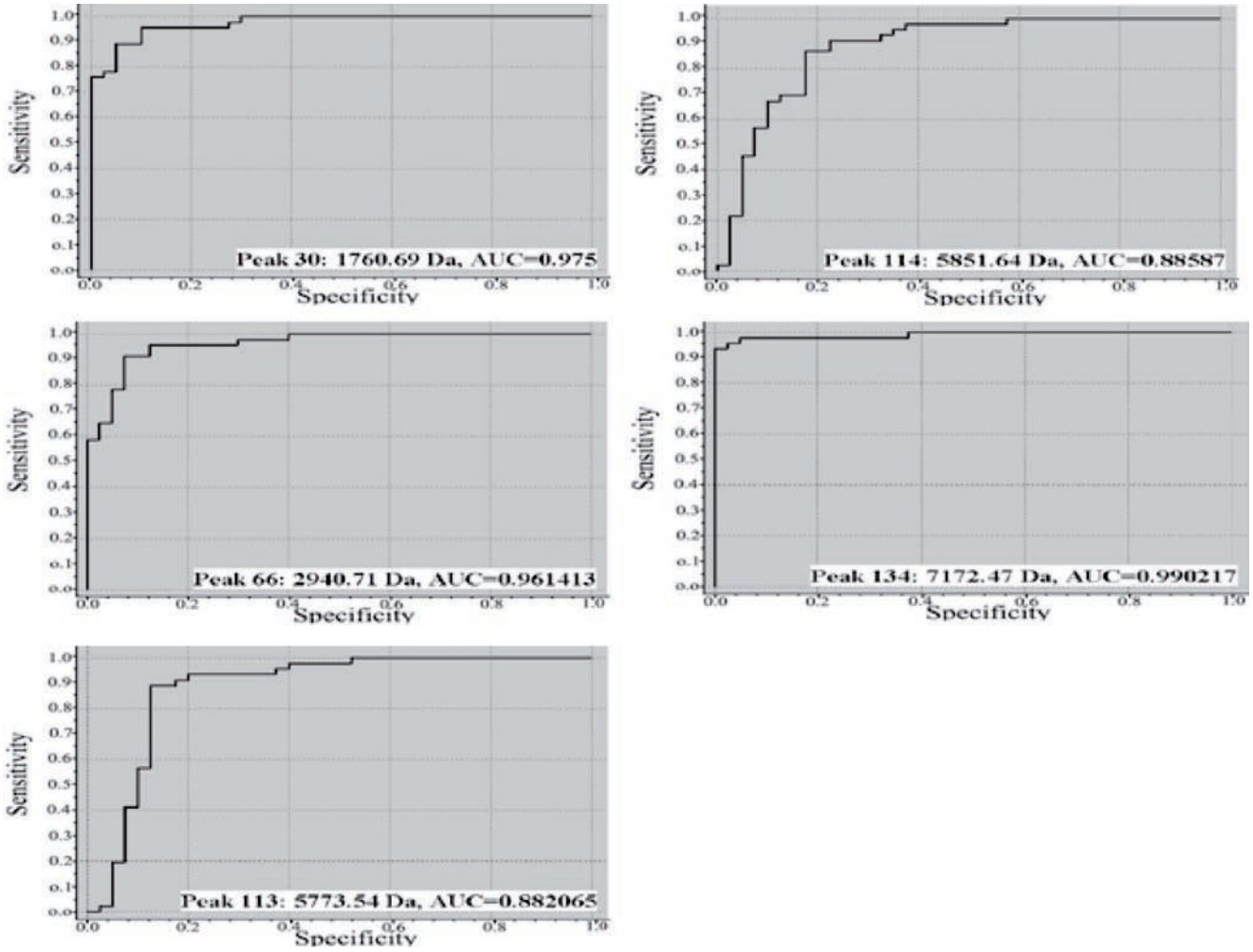

Figure 2. Receiver operating characteristic (ROC) curve with area under the curve values of the differentiable peaks.

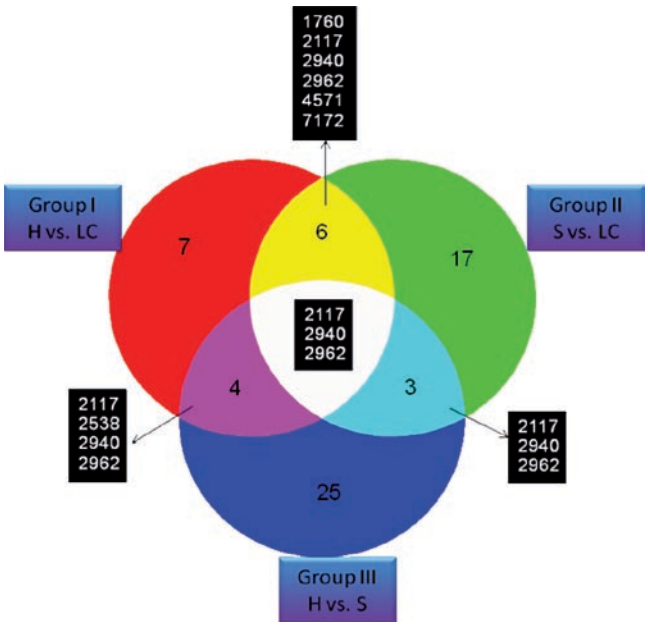

Figure 3. Venn diagram showing the overlapping of the model peaks for groups I, II, and III.

level 0.5097 in group II, hence this peak would not be considered as a signature peptide. Although the peak at *m/z* 2117 Da has a significant AUC value, it is inconsistent throughout the spectrum. Therefore, peak at *m/z* 2940 Da along with two other peaks at *m/z* 1760 and 7172 Da that were included in the classification model for groups I, II, and IV, generated on the basis of SVM and SNN algorithm showed highly discriminating ability $p < 10^{-6}$ and AUC in the range of 0.7956–0.9923 for groups I and II. In addition to these three highly differentiable peaks picked by the model, there was an additional pattern in the mass range of *m/z* 5500–5900 Da, which were not included in the model but have the most discriminatory power with low *p* value (<0.001) and high AUC of around 0.8809–0.9418. Differentiated signature protein/peptide pattern consisted of five peaks at *m/z* 1760, 2940, 5773, 5851, and 7172 Da (Figure 4). Among these differential peaks, three peaks at *m/z* 1760, 5773, and 5851 Da were over expressed and were only observed in LC patients, while peaks at *m/z* 2940 and 7172 Da were under expressed and showed a sequential decrease from NS to S and then to LC patients. The propagation rate of these peaks could be observed in Figure 5, which clearly showed that smoking is an intermediary stage between

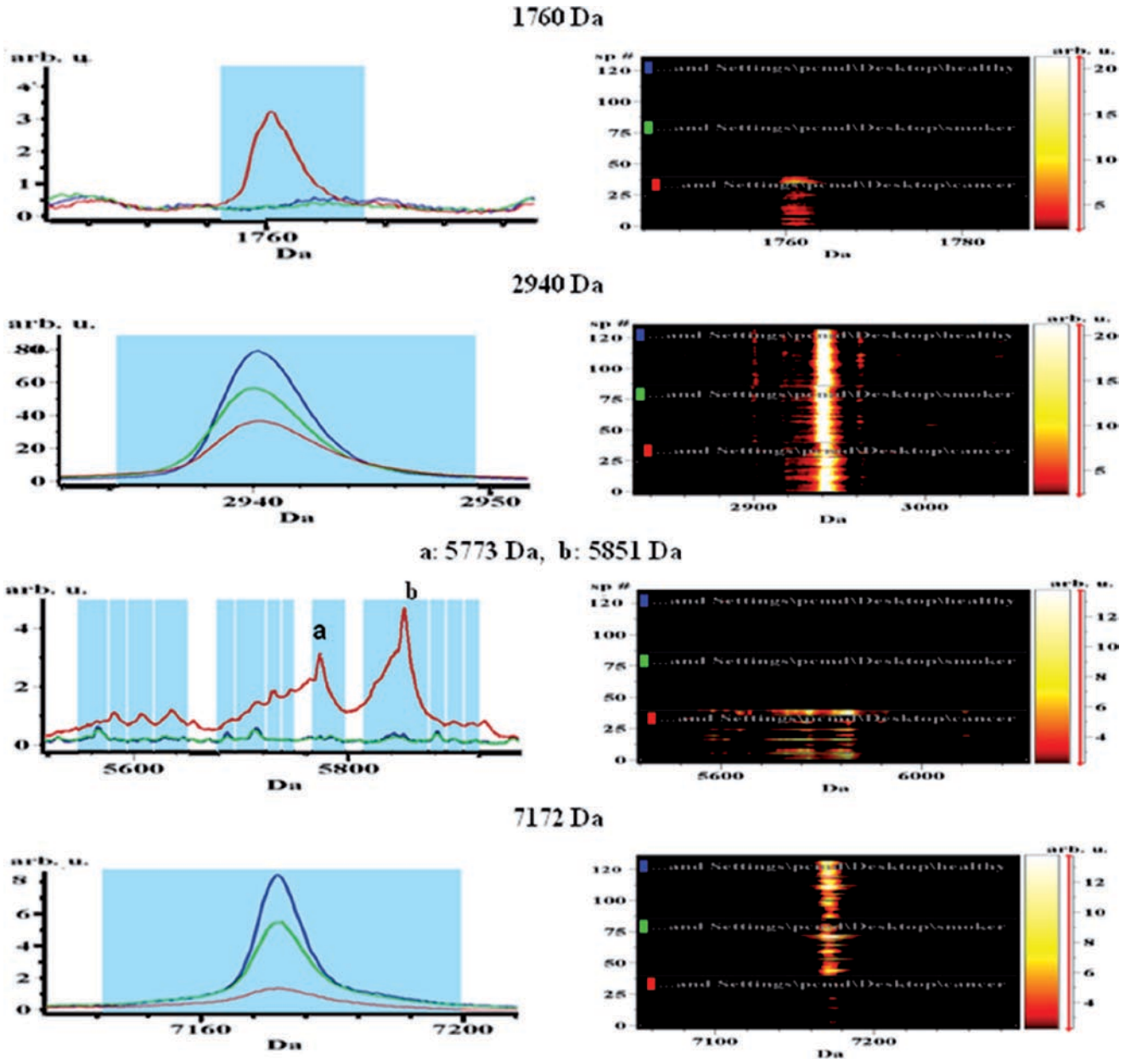

Figure 4. Differentially expressed peaks: Gel view in chromatic mode representing the comparison of average intensity of the individual signature peptide. Lung cancer (red), smokers (green), and nonsmokers (blue).

healthy and LC. Similar picture was observed in the box and whiskers plot. Further analysis of the most valuable peaks, done by the two-dimensional peak distribution views, indicated standard deviation of the class average of the peak areas. A plot of *m/z* 1760 Da with other discriminatory peaks of the model *m/z* 2940 and 7172 Da showed that LC was clearly distinguishable from the two classes. These characteristic peptides not only observed in the average spectra but these changes could also be monitored in individual spectra of the three classes, that is, LC, S, and NS (See Supplementary Data Table 6, Figures 3–5).

Recently, a number of studies have been conducted utilizing the magnetic bead approach for different malignancies. Shevchenko et al. (2010) utilized WCX beads for the determination of signature peptides for small cell lung carcinoma and showed distinctive peptide pattern. Similar work has also been done by Lin et al. (2010) utilizing the same WCX magnetic bead coupled with MALDI-TOF MS approach for the detection of lung adenocarcinoma. Jacot et al. (2008) identified and showed a list of 88 differentially expressed markers by serum proteomic profiling of LC in high-risk groups. Among these, 88 differentially expressed markers, a peak at *m/z* 7172 Da has been shown to be under expressed in LC compared with other chronic lung disease, a result that is consistent with our findings. They have reported this peak with an AUC value of 0.814, while in our study, we found an AUC of 0.9902–0.9500 in groups I and II, respectively. Moreover, a

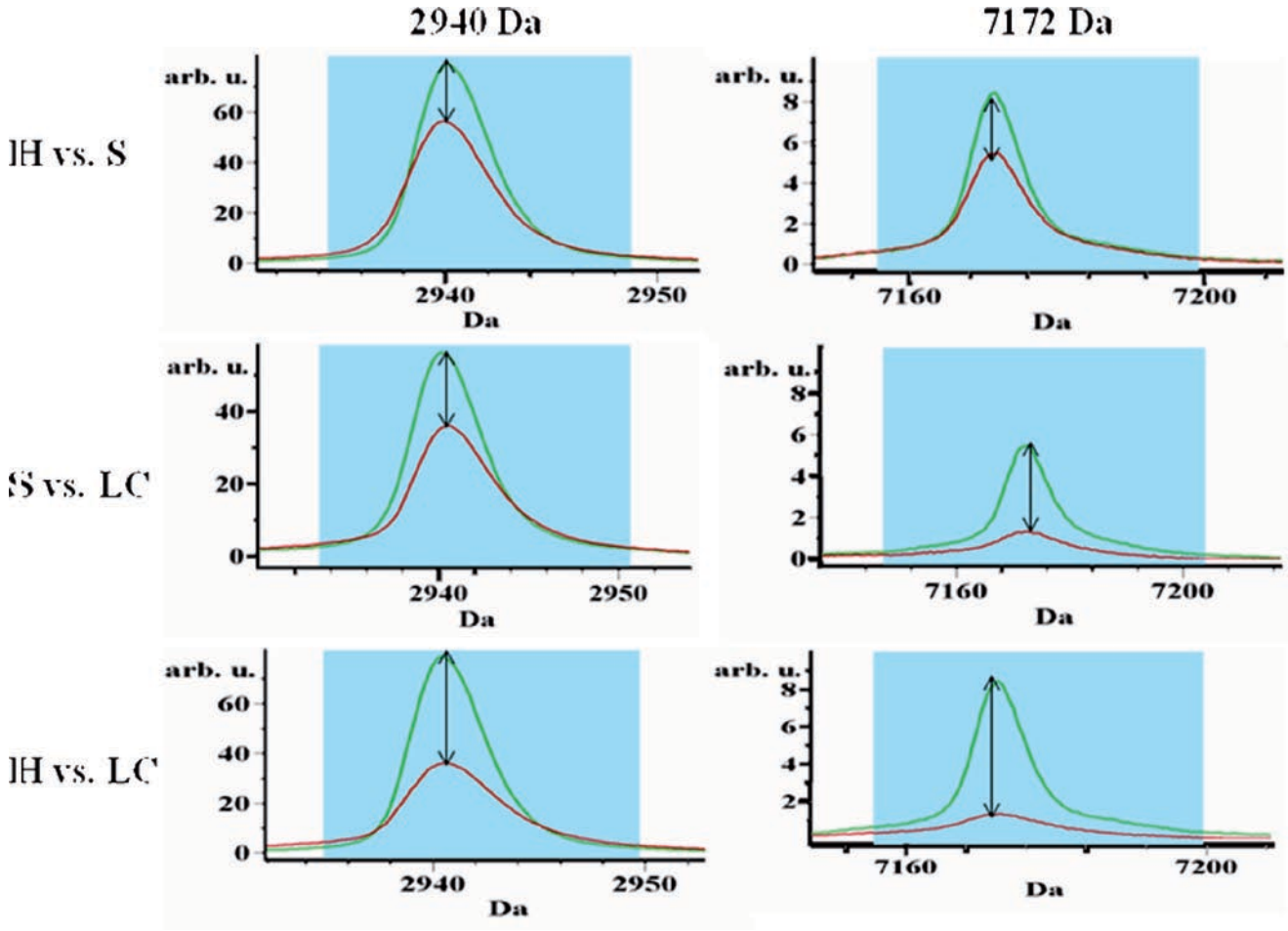

Figure 5. Average intensity difference graph for the two most differentiable peaks among the groups. Green: nonsmokers, red: smokers/lung cancer.

similar protocol has been investigated for other cancers included ovarian, colorectal, and bladder cancer (Fan et al. 2010, Liu et al. 2011, Schwamborn et al. 2009). The peak at *m/z* 1760 Da was absent in others despite the use of the same magnetic bead approach, indicating that this signature peptide is specific for LC. The MS-based profiling often shows proteins/peptides related to inflammatory processes, able to distinguish healthy from diseased samples, while the biomarker discovery, involving the identification of molecules, leads also to the understanding of disease pathophysiology. Therefore, both approaches have limitations and advantages.

One-dimensional SDS-PAGE of Dynabead flow through and Dynabead eluate was also carried out to evaluate the enrichment capacity of Dynabeads. The gel clearly showed that Dynabeads capture mainly the less abundant proteins/peptides and the high abundant proteins/peptides specifically albumin were removed in the flow through (See Supplementary Data Figure 6). Therefore, the magnetic bead approach can be used as an efficient fractionation technique for the removal of high molecular weight proteins. This study can be further improved by including a greater number of samples, other lung diseases as a control, and the characterization of distinctive peaks.

Conclusion

In conclusion, pattern-based profiling of plasma peptides in LC patients, and healthy S and NS by RPC-18 magnetic bead fractionation and coupled with MALDI-TOF-MS technique has been developed. Findings showed many characteristic peaks and provided a differentiated pattern among the groups. Detailed statistical evaluation and developed model showed up- or down-regulation in the intensities of marker peaks with high diagnostic capability and therefore can be served as a potential tool for efficient screening of LC patients with high sensitivity and specificity.

Acknowledgments

Thanks to the staff of JPMC and Diagnostic laboratory (PCMD) for their assistance in blood collection. Thanks to all volunteers involved in this study and Prof. Dr. Daniel Hoessli for reading this article and for providing useful suggestions. Thanks to Mr. Arslan Ali, Mr. Safdar,

Miss Amna Jabbar, Miss Shulmaila Mazhar, and Miss Mahwish Saleem (ICCBS) for their assistance in statistical analysis.

Declaration of interest

The authors report no conflict of interest.

References

Chang JT, Chen LC, Wei SY, Chen YJ, Wang HM, Liao CT. (2006). Increase diagnostic efficacy by combined use of fingerprint markers in mass spectrometry-plasma peptidomes from nasopharyngeal cancer patients for example. *Clin Biochem* 39:1144–1151.

Cheng AJ, Chen LC, Chien KY, Chen YJ, Chang JTC, Wang HM. (2005). Oral cancer plasma tumor marker identified with bead-based affinity-fractionated proteomic technology. *Clin Chem* 51:2236–2244.

Fan DM, Shi HR, Chen ZM, Wu QH, Liu HN, Zhang RT. (2010). Early detection of ovarian carcinoma by proteome profiling based on magnetic bead separation and matrix-assisted laser desorption/ionization time of flight mass spectrometry. *Afr J Microbiol Res* 4:940–951.

Flanagan N. (2007). Magnetic beads for biomarker discovery. *Genetic Eng Biotech News* 27: [Online] Available at: http://www.genengnews.com/gen-articles/magnetic-beads-for-biomarker-discovery/2167/

Freed GL, Cazares LH, Fichandler CE, Fuller TW, Sawyer CA, Stack BC, Schraff S, Semmes OJ, Trad WJ, Drake RR. (2008). Differential capture of serum proteins for expression profiling and biomarker discovery in pre- and post treatment head and neck cancer samples. *Laryngoscope* 18:61–68.

Goldman R, Ressom HW, Abdel-Hamid M, Goldman L, Wang A, Varghese RS, An Y, Loffredo CA, Drake SK, Eissa SA, Gouda I, Ezzat S, Moiseiwitsch FS. (2007). Candidate markers for the detection of hepatocellular carcinoma in low-molecular weight fraction of serum. *Carcinogenesis* 28:2149–2153.

GLOBOCAN 2008, IARC, 2010 - GLOBOCAN: Country Fast Stat http://globocan.iarc.fr/factsheets/populations/factsheet.asp?uno=586

Jacobs DR, Adachi H, Mulder I, Kromhout D, Menotti A, Nissinen A, Blackburn H. (1999). Cigarette smoking and mortality risk: Twenty-five-year follow-up of the seven countries study. *Arch Intern Med* 159:733–740.

Jacot W, Lhermitte L, Dossat N, Pujol JL, Molinari N, Daurès JP, Maudelonde T, Mangé A, Solassol J. (2008). Serum proteomic profiling of lung cancer in high-risk groups and determination of clinical outcomes. *J Thorac Oncol* 3:840–850.

Jemal A, Center MM, DeSantis C, Ward EM. (2010). Global patterns of cancer incidence and mortality rates and trends. *Cancer Epidemiol Biomarkers Prev* 19:1893–1907.

Jimenez CR, Filali ZE, Knol JC, Hoekman K, Kruyt FAE, Giaccone G, Smit AB, Li KW. (2007). Automated serum peptide profiling using novel magnetic C18 beads off-line coupled to MALDI-TOF-MS. *Proteomics Clin Appl* 1:598–604.

Lin XL, Yang SY, Du J, Tian YX, Bu LN, Huo SF, Wang FP, Nan YD. (2010). Detection of lung adenocarcinoma using magnetic beads based matrix-assisted laser desorption/ionization time-of-flight mass spectrometry serum protein profiling. *Chin Med J* 123:34–39.

Liu C, Pan C, Shen J, Wang H, Yong L. (2011). MALDI-TOF MS combined with magnetic beads for detecting serum protein biomarkers and establishment of boosting decision tree model for diagnosis of colorectal cancer. *Int J Med Sci* 8:39–47.

Mascaux C, Peled N, Garg K, Kato Y, Wynes MW, Hirsch FR. Early detection and screening of lung cancer. (2010). *Expert Rev Mol Diagn* 10:799–815.

Orvisky E, Drake SK, Martin BM, Abdel-Hamid M, Ressom HW, Varghese RS, An Y, Saha D, Hortin GL, Loffredo CA, Goldman R. (2006). Enrichment of low molecular weight fraction of serum for MS analysis of peptides associated with hepatocellular carcinoma. *Proteomics* 6:2895–2902.

Proctor RN. Tobacco and the global lung cancer epidemic. (2001). *Nat Rev Cancer* 1:82–86.

Rai AJ, Gelfand CA, Haywood BC, Warunek DJ, Yi J, Schuchard MD, Mehigh RJ, Cockrill SL, Scott GB, Tammen H, Schulz-Knappe P, Speicher DW, Vitzthum F, Haab BB, Siest G, Chan DW. (2005). HUPO Plasma Proteome Project specimen collection and handling: towards the standardization of parameters for plasma proteome samples. *Proteomics* 5:3262–3277.

Sasco AJ, Secretan MB, Straif K. (2004). Tobacco smoking and cancer: a brief review of recent epidemiological evidence. *Lung Cancer* 45:3–9.

Schwamborn K, Krieg RC, Grosse J, Reulen N, Chen RW, Knuechel R, Jakse G, Henkel C. (2009). Serum proteomic profiling in patients with bladder cancer. *Eur Urol* 56:989–996.

Shevchenko VE, Aronotskaya NE, Zaridze DG. (2010). Detection of lung cancer using plasma protein profiling by matrix- assisted laser desorption/ionization time-of-flight mass spectrometry. *Eur J mass spectrum (Chichester En.)* 16:539–549.

Sven B, Uta C, Georg MF, Jan L, Alexander L, Joachim T. (2005). Standardized approach to proteome profiling of human serum based on magnetic bead separation and matrix-assisted laser desorption/ionization time of flight mass spectrometry. *Clin Chem* 51:973–988.

Villanueva J, Martorella AJ, Lawlor K, Philip J, Fleisher M, Robbins RJ, Tempst P. (2006a). Serum peptidome patterns that distinguish metastatic thyroid carcinoma from cancer-free controls are unbiased by gender and age. *Mol Cell Proteomics* 5:1840–1852.

Villanueva J, Philip J, Entenberg D, Chaparro CA, Tanwar MK, Holland EC, Tempst P. (2004). Serum peptide profiling by magnetic particle-assisted, automated sample processing and MALDI-TOF mass spectrometry. *Ana Chem* 76:1560–1570.

Villanueva J, Shaffer DR, Philip J, Chaparro CA, Erdjument-Bromage H, Olshen AB. (2006b). Differential exoprotease activities confer tumor-specific serum peptidome patterns. *J Clin Invest* 116:271–284.

Walser T, Cui X, Yanagawa J, Lee JM, Heinrich E, Lee G, Sharma S, Dubinett SM. (2008). Smoking and lung cancer. The role of inflammation. *Proc Am Thorac Soc* 5:811–815.

Wong MYM, Yu KOY, Poon TCW, Ang IL, Law MK, Chan KYW, Ng EWY, Ngai SM, Sung JJY, Chan HLY. (2010). Magnetic bead-based serum proteomic fingerprinting method for parallel analytical analysis and micro preparative purification. *Electrophoresis* 31: 1721–1730.

Yildiz PB, Shyr Y, Rahman JS, Wardwell NR, Zimmerman LJ, Shakhtour B, Gray WH, Chen S, Li M, Roder H, Liebler DC, Biqbee WL, Sieqfried JM, Weissfeld JL, Gonzalez AL, Ninan M, Johnson DH, Carbone DP, Caprioli RM, Massion, PP. (2007). Diagnostic accuracy of MALDI mass spectrometric analysis of unfractionated serum in lung cancer. *J Thorac Oncol* 2:893–901.